

Determination of Transport and Thermal Properties of Silicon Samples by the Phase-Lag and Sf/Sr Methods

Łukasz CHROBAK, Mirosław MALIŃSKI

Technical University of Koszalin
Faculty of Electronics and Computer Science
Śniadeckich 2, 75-453 Koszalin, Poland
e-mail: lukasz.chrobak@tu.koszalin.pl

(received October 20, 2008; accepted November 11, 2009)

The paper presents results of photoacoustic studies of thermal and transport properties of silicon samples. It shows for the first time the influence of plasma waves on the *Sf/Sr* and phase-lag frequency photoacoustic characteristics and describes a procedure leading to the determination of both thermal diffusivity and the life time or the diffusion length of excess carriers from those characteristics.

Keywords: photoacoustic methods, semiconductors, silicon parameters.

1. Introduction

Thermal diffusivity of semiconductor samples is one of the basic thermal parameters used in photoacoustics. Correctness of its determination influences the determination of other physical parameters extracted from photoacoustic experiments. The most popular methods of its determination are the *Sf/Sr* and phase-lag ones. The *Sf/Sr* method means that the ratio of the amplitudes of the photoacoustic signal in front and rear configurations as functions of frequency of modulation are measured. The phase-lag method means that the phase difference between the photoacoustic signals in the front and rear configuration is measured [1].

These methods were elaborated for samples in which the thermal diffusion process is the only one in the investigated samples. An analysis of those methods for case when the drum effect is also taken into account was presented in paper [2]. Further investigations of the processes involved in the photoacoustic effect indicated that the diffusion of the excess carriers plays an essential role in the generation of the photoacoustic signal in Ge crystals too [3, 4]. The plasma wave effect in silicon was described in paper [5].

The thermal diffusivity is essential for, among other things, computations of the temperature spatial distribution in the sample [6] and for the correct interpretation of the photoacoustic spectra [7, 8]. Furthermore, the choice of the appropriate mathematical model describing the photoacoustic signal is equally important.

This paper shows that the Sf/Sr and phase-lag frequency characteristics also bring information on the recombination parameters when the plasma wave effect is considered in the photoacoustic model and the latter can not be neglected. This information can be extracted from the shape of the Sf/Sr and phase-lag frequency characteristics.

This paper also demonstrates the influence of the plasma wave effect on these characteristics. The theoretical characteristics are confirmed by appropriate experimental characteristics obtained for silicon samples exhibiting long life time of optically generated excess carriers.

2. Experimental procedure

The experimental characteristics presented in this paper were measured by the conventional photoacoustic set-up (Fig. 1). The same set-up has been used for the measurements described in paper [9].

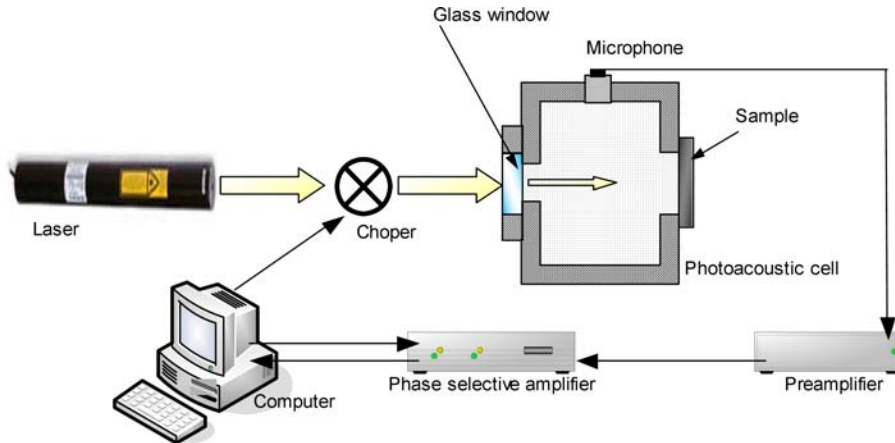


Fig. 1. Schematic diagram of the experimental set-up used in the measurements.

It consisted of the green (532 nm) semiconductor laser (model SDL-532-030T), which was the source of the intensity-modulated beam of light in the range of frequencies from 5 Hz to 1 kHz. The electret microphone was the detector of the photoacoustic signal that was measured by the phase selective method of detection with a lock-in amplifier (Scitec Instruments 500 MC). The measurements were computer controlled. The samples were prepared in the way that one side of the sample was polished (mirror type) while the other one was roughened (matt

type). A schematic diagram of the experimental configuration of the sample in the photoacoustic cell is presented in Fig. 2.

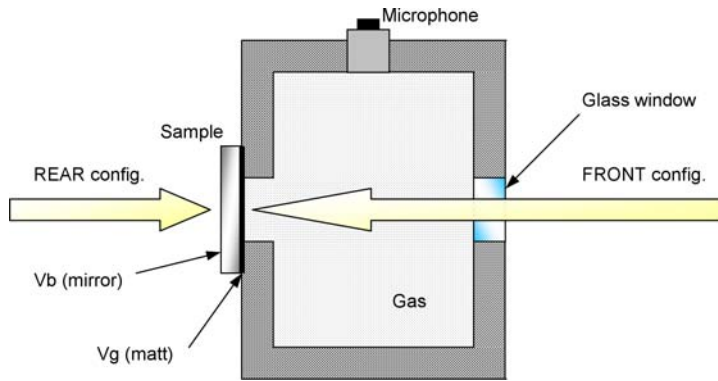


Fig. 2. Schematic diagram of the sample mounted in the photoacoustic cell.

3. Theory

For samples exhibiting short lifetime of excess carriers, the S_f/S_r and phase-lag characteristics are described respectively by the formulae (1)–(3):

$$\frac{S_f}{S_r} = \left[\cosh^2 \left(\frac{d}{\mu} \right) - \sin^2 \left(\frac{d}{\mu} \right) \right]^{1/2}, \quad (1)$$

$$\text{PhaseLag} = a \tan \left[\tanh \left(\frac{d}{\mu} \right) \tan \left(\frac{d}{\mu} \right) \right], \quad (2)$$

$$\mu = \left[\frac{\alpha}{\pi f} \right]^{1/2}, \quad (3)$$

where d is the thickness of the sample and α is the thermal diffusivity.

The example of the theoretical S_f/S_r and phase-lag characteristics for different values of thermal diffusivities are presented in Fig. 3.

Computations of the photoacoustic S_f/S_r and phase-lag characteristics with contribution of the plasma wave effect were performed in the compact plasma wave model [10]. The PA signals measured in the front and rear configurations are given by the formulae (4)–(13).

$$T_T(x, f, \alpha, \tau, D) = \frac{(E - Eg) I_0 \beta}{2E\kappa\sigma(1 - e^{-2\sigma d})} \left[\int_0^x e^{-\beta z} W1(z, x) dz + \int_x^d e^{-\beta z} W2(z, x) dz \right], \quad (4)$$

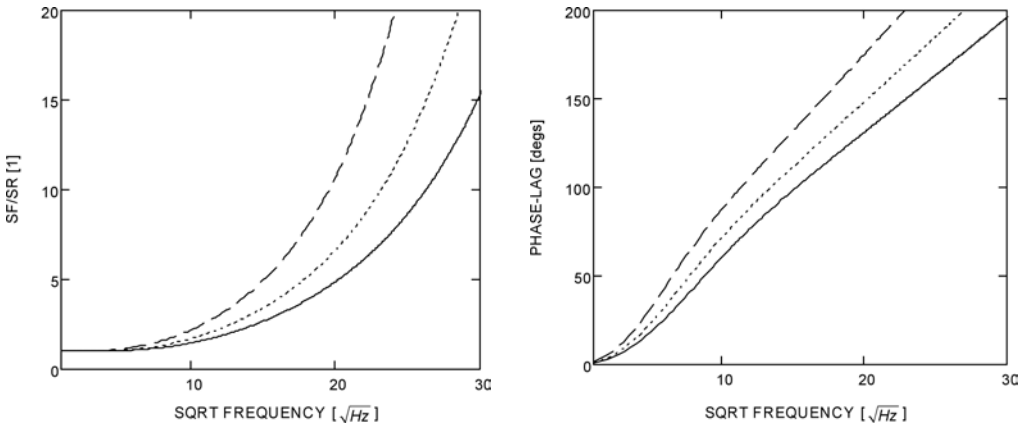


Fig. 3. Theoretical Sf/Sr and phase-lag characteristics versus the frequency of modulation for three different values of thermal diffusivity: solid line – $\alpha_1 = 0.9 \text{ cm}^2/\text{s}$, dotted line – $\alpha_2 = 0.7 \text{ cm}^2/\text{s}$, dashed line – $\alpha_3 = 0.5 \text{ cm}^2/\text{s}$; thickness of the sample $d = 0.061 \text{ cm}$.

$$T_{VR}(x, f, \alpha, \tau, V_g, V_b, D) = \frac{EgI_0}{\kappa\sigma\tau(1 - e^{-2\sigma d})} \left[\int_0^x \delta n(z) W1(z, x) dz + \int_x^d \delta n(z) W2(z, x) dz \right], \quad (5)$$

$$T_{SR}(x, f, \alpha, \tau, V_g, V_b, D) = \frac{EgI_0}{\kappa\sigma(1 - e^{-2\sigma d})} [V_g\delta n(0) W1(0, x) + V_b\delta n(d) W2(d, x)], \quad (6)$$

$$W1(z, x) = e^{-\sigma(x-z)} + e^{-\sigma(2d-z-x)} + e^{-\sigma(z+x)} + e^{-\sigma(2d+z-x)}, \quad (7)$$

$$W2(z, x) = e^{-\sigma(z-x)} + e^{-\sigma(z+x)} + e^{-\sigma(2d-z-x)} + e^{-\sigma(2d-z+x)}, \quad (8)$$

$$P(0, f, \alpha, \tau, V_g, V_b, D) = \frac{T_T(0, f, \alpha, \tau, D) + T_{VR}(0, f, \alpha, \tau, V_g, V_b, D) + T_{SR}(0, f, \alpha, \tau, V_g, V_b, D)}{\sigma(f, \alpha)}, \quad (9)$$

$$P(d, f, \alpha, \tau, V_b, V_g, D) = \frac{T_T(d, f, \alpha, \tau, D) + T_{VR}(d, f, \alpha, \tau, V_b, V_g, D) + T_{SR}(d, f, \alpha, \tau, V_b, V_g, D)}{\sigma(f, \alpha)}, \quad (10)$$

$$\sigma(f, \alpha) = (1 + i) \left(\frac{\pi f}{\alpha} \right)^{1/2}, \quad (11)$$

$$\frac{Sf}{Sr} = \frac{\text{Amp}(P(0, f, \alpha, \tau, V_g, V_b, D))}{\text{Amp}(P(d, f, \alpha, \tau, V_b, V_g, D))}, \quad (12)$$

$$\text{PhaseLag} = \text{Phase}(P(0, f, \alpha, \tau, V_g, V_b, D)) - \text{Phase}(P(d, f, \alpha, \tau, V_b, V_g, D)), \quad (13)$$

where x is the spatial coordinate of the sample, τ is the life time of excess carriers, α is the thermal diffusivity, d is the thickness of the sample, V_g velocity of the matt surface recombination, V_b velocity of the mirror surface recombination, D is the diffusion coefficient of the carriers, E is the energy of absorbed photons, β is the optical absorption coefficient, T_T is the thermal contribution resulting from the intraband relaxation of the carriers, T_{VR} – is the volume recombination and T_{SR} the surface recombination thermal contributions to the total temperature distribution in the sample.

An example of the theoretical Sf/Sr and phase-lag characteristics with the contribution of the plasma wave effect calculated by a compact model for different thermal diffusivities are presented in Fig. 4. The parameters taken for the calculation were: $\tau = 80 \mu\text{s}$, $\alpha = 0.5, 0.7, 0.9 \text{ cm}^2/\text{s}$, $d = 0.061 \text{ cm}$, $V_g = 1500 \text{ cm/s}$, $V_b = 100 \text{ cm/s}$, $D = 15 \text{ cm}^2/\text{s}$, $E = 2.0 \text{ eV}$, $\beta = 1000 \text{ cm}^{-1}$.

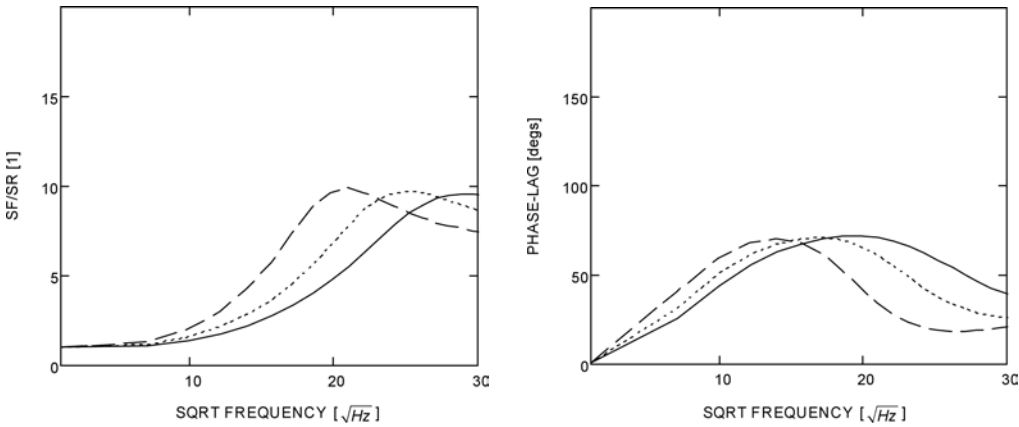


Fig. 4. Theoretical Sf/Sr and phase-lag characteristics with the contribution of the plasma wave effect versus the frequency of modulation for three different values of the thermal diffusivity: solid line – $\alpha_1 = 0.9 \text{ cm}^2/\text{s}$, dotted line – $\alpha_2 = 0.7 \text{ cm}^2/\text{s}$, dashed line – $\alpha_3 = 0.5 \text{ cm}^2/\text{s}$.

4. Experimental results

The experimental and theoretical Sf/Sr and phase-lag frequency characteristics of the first sample are presented in Fig. 5.

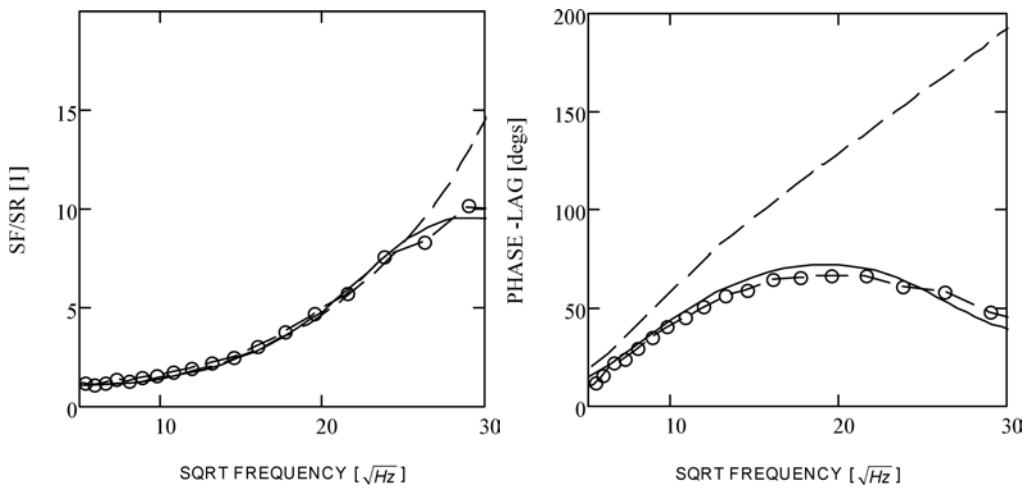


Fig. 5. Theoretical and experimental Sf/Sr and phase-lag characteristics. Dash lines are the only theoretical characteristics of the thermal effect T_T , solid lines are characteristics of the thermal effect with the plasma wave contribution, circles are experimental points.

The theoretical curves were computed for the following set of experimental and fitting parameters: $\tau = 80 \mu\text{s}$, $\alpha = 0.9 \text{ cm}^2/\text{s}$, $d = 0.061 \text{ cm}$, $V_g = 1500 \text{ cm/s}$, $V_b = 100 \text{ cm/s}$, $D = 15 \text{ cm}^2/\text{s}$, $E = 2.0 \text{ eV}$, $\beta = 1000 \text{ cm}^{-1}$, $Le = (D\tau)^{0.5} = 0.035 \text{ cm}$ is the diffusion length of the carriers.

For comparison, the theoretical curves computed for $\tau = 8 \mu\text{s}$ and $\alpha = 0.9 \text{ cm}^2/\text{s}$ are presented in Fig. 6.

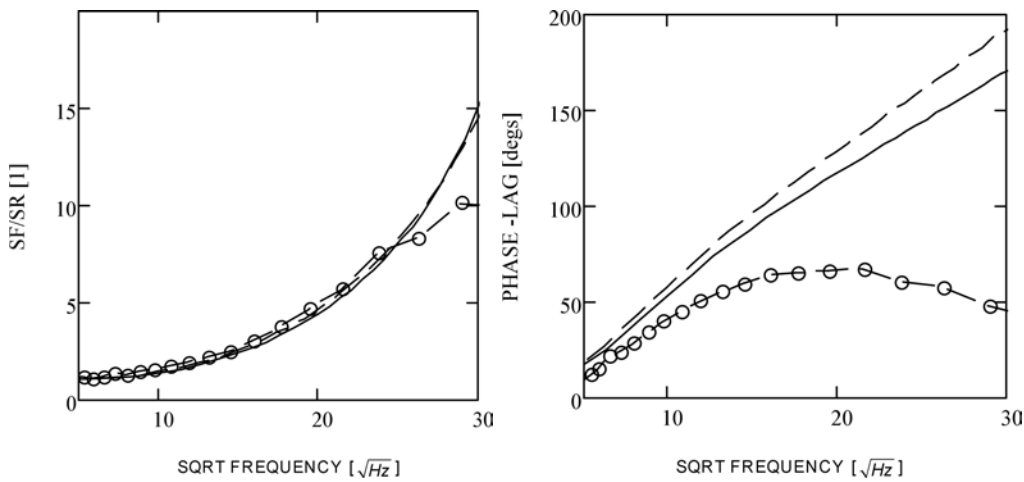


Fig. 6. Theoretical and experimental Sf/Sr and phase-lag characteristics. Dash lines are the only theoretical characteristics of the thermal effect T_T , solid lines are characteristic of the thermal effect with the plasma wave contribution, circles are experimental points.

The theoretical characteristics computed for $\tau = 8 \mu\text{s}$ and $\alpha = 0.6 \text{ cm}^2/\text{s}$ are shown in Fig. 7.

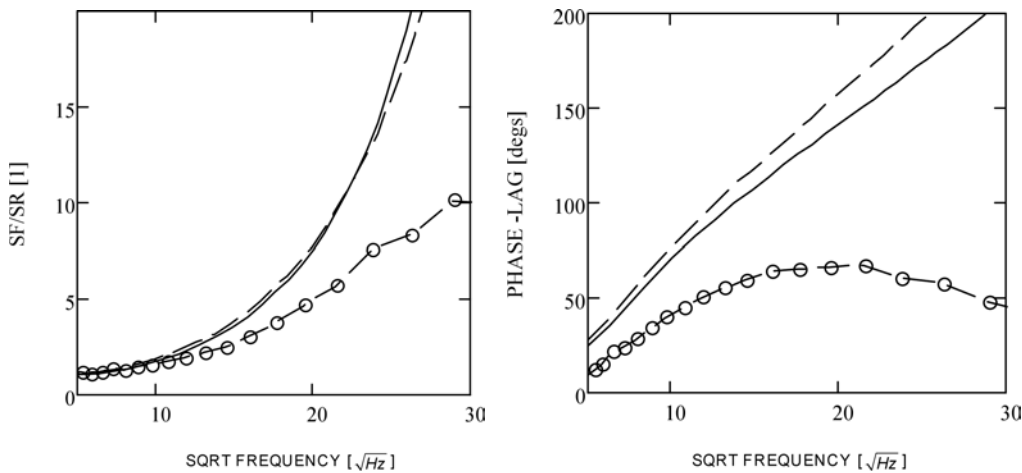


Fig. 7. Theoretical and experimental Sf/Sr and phase-lag characteristics. Dash lines are the only theoretical characteristics of the thermal effect T_T , solid lines are characteristic of the thermal effect with the plasma wave contribution, circles are experimental points.

5. Conclusions

Conclusions drawn from the above characteristics are the following ones. For case when the matt surface is in the photoacoustic cell and the mirror side of the sample is outside the photoacoustic cell, the Sf/Sr characteristics depends mainly on the thermal diffusivity of the sample and are much less sensitive to the life times of the carriers, at least for the investigated range of frequencies. The phase lag characteristics depends mainly on the life time of carriers and depends practically much weaker on the thermal diffusivity of the material.

For the proper determination of the thermal and transport properties of semiconductor samples, both the Sf/Sr and phase-lag characteristics should be analyzed for the same set of fitting parameters. It is suggested that the thermal diffusivity should be determined from the Sf/Sr characteristics and next, the lifetimes of excess carriers should be extracted from the fitting to the phase-lag characteristics for the determined values of the thermal diffusivity. The diffusion length of the carriers can be estimated as $Le = (D\tau)^{1/2}$. The thermal diffusivity of silicon samples or other semiconductor materials, can be determined properly from the phase lag only for short lifetimes of excess carriers $\tau < 1 \mu\text{s}$ for frequencies $f < 1 \text{ kHz}$ when the thermal wave model is correct. For longer lifetimes of carriers, the plasma wave effect must be taken into account and the fitting of theoretical curves to the experimental characteristics must be performed by the plasma wave model of a photoacoustic signal.

References

- [1] PESSOA O. JR., CESAR C.L., PATEL N.A., VARGAS H., GHIZONI C.C., MIRANDA L.C.M., *Two-beam photoacoustic phase measurement of the thermal diffusivity of solids*, J. Appl. Phys., **59**, 4, 1316 (1986).
- [2] SUSZYŃSKI Z., MALIŃSKI M., BYCHTO L., *Photoacoustic measurements of the thermal diffusivity of solids in the presence of a drum effect*, Archives of Acoustics, **22**, 3, 343–349 (1997).
- [3] DRAMICANIN M.D., RISTOVSKI Z.D., NICOLIC P.M., VASILJEVIC D.G., TODOROVIC D.M., *Photoacoustic investigation of transport in semiconductors: Theoretical and experimental study of a Ge single crystal*, Physical Review, **B 51**, 20, 14226 (1995).
- [4] TODOROVIC D.M., NIKOLIC P.M., *Investigation of carrier transport processes in semiconductors by the photoacoustic frequency transmission method*, Opt. Eng., **36**, 2, 432 (1997).
- [5] MARIN E., REICH I., DIAZ P., VARGAZ H., *Influence of carrier recombination on the thermodiffusion, thermoelastic and electronic strain photoacoustic signal generation mechanism in semiconductors*, Anal. Sci., **17**, 284 (2001).
- [6] MALIŃSKI M., *Temperature distribution formulae – Applications in photoacoustics*, Archives of Acoustics, **27**, (3), 217–228 (2002).
- [7] MALIŃSKI M., MEMON A., IKARI T., *Interpretation of the photoacoustic piezoelectric spectra of p-type silicon samples*, Archives of Acoustics, **28**, 2, 139–148 (2003).
- [8] MALIŃSKI M., *Numerical analysis of piezoelectric photoacoustic spectra*, Archives of Acoustics, **28**, 1, 43–58 (2003).
- [9] MALIŃSKI M., CHROBAK Ł., PATRYN A., *Theoretical and experimental studies of a plasma wave contribution to the photoacoustic signal for Si samples*, Acta Acustica United With Acustica, **95**, 60–64 (2009).
- [10] BYCHTO L., MALIŃSKI M., *Comparison of plasma wave models in photoacoustics*, J. Phys. IV France, **129**, 213 (2005).